

BPC 01265

The structure of a membrane-spanning polypeptide studied by molecular dynamics

Olle Edholm^a and Fritz Jähnig^b

^a Department of Theoretical Physics, Royal Institute of Technology, S-10044 Stockholm 70, Sweden
and ^b Max-Planck-Institut für Biologie, Corrensstrasse 38, D-7400 Tübingen, F.R.G.

Received 19 October 1987

Revised manuscript received 18 March 1988

Accepted 30 March 1988

Glycophorin; Hydrophobic effect; Membrane-spanning helix; Thermal fluctuation; Molecular dynamics

We have performed a molecular dynamics simulation of a 46-residue segment of glycophorin which includes the hydrophobic membrane-spanning region of this protein. The presence of a membrane and of water is taken into account in a continuum approximation which makes use of phenomenological hydrophobic energies. The initial α -helical conformation and the membrane incorporation of the hydrophobic segment remain stable for the length of the simulation which is 100 ps. Moreover, when the hydrophobic segment is partially shifted out of the membrane, it moves back into the membrane. Superimposed on these deterministic effects one also observes thermal fluctuations in the form of bending and tilting of the membrane-spanning helix.

1. Introduction

There is an ever-growing need to calculate the three-dimensional structure of proteins from their amino acid sequence. For soluble proteins, the number of possible structures which have to be compared in order to determine the one of lowest energy is too large for the problem to be solved on present-day computers. For membrane proteins, the situation may be more favorable, the point being that the lipid bilayer imposes severe restrictions on the folding of the protein. Firstly, protein segments spanning the bilayer in contact with the lipids must be hydrophobic or at least amphipathic, i.e., have at least one hydrophobic side. Secondly, these segments must be in an α -helix or β -strand conformation for the hydrogen bonds to be saturated. A membrane-spanning α -helix com-

prises about 20 residues, a β -strand about 10. Hence, all one has to do to predict the topology of a membrane protein is to search its sequence for stretches of 10 or 20 hydrophobic residues or, more generally, of periodic amphipathy [1,2]. What remains unknown with this approach is the lateral arrangement of the α -helices or β -strands in the plane of the membrane. This reduced problem might be solved by means of molecular dynamics (MD) simulations on fast computers.

MD simulations have been performed on soluble proteins with the X-ray structure or NMR results as input data [3,4]. Most of the simulations were carried out in vacuum, but sometimes water molecules were added [5]. In the case of membrane proteins, it is evident that lipid molecules must also be included. Lipid molecules alone forming a bilayer have already been simulated [6] and also a simulation of an α -helix in a bilayer of 100 lipid molecules is available [7]. In principle, water molecules might be added and the protein/lipid/water system be treated on a molecular

Correspondence address: O. Edholm, Department of Theoretical Physics, Royal Institute of Technology, S-10044 Stockholm 70, Sweden.

level. This would be time-consuming, but could be done. The result, however, would not be very reliable. The reason is that the hydrophobic effect, which to a large extent determines the folding of a membrane protein, results from the small difference between the strong interactions of the atoms of a protein with water and lipid. These interactions are partially of entropic origin, arising from the reduction of the mobility of water and lipid molecules at the surface of proteins, and partially of energetic origin, resulting from electrostatic, van der Waals and hydrogen bond interactions [8,9]. To calculate this difference correctly would require a better water model than is presently available. Simulations of pure water gave too low a dielectric constant [10], and simulations of water with krypton atoms dissolved showed no tendency of them to aggregate which contradicts the conventional picture of the hydrophobic effect [11]. Also, a fatty acid micelle in water did not adopt a reasonable shape until the charge of the fatty acid molecules was reduced by a factor of 2 [12]. Thus, the hydrophobic effect of a membrane protein, at present, cannot be described satisfactorily by including lipid and water on a molecular level.

Under these circumstances, we attempted to develop a continuum approximation for the hydrophobic effect which is based on phenomenological energies. Our approach is still a vacuum simulation but with an external potential to account for the lipid/water interface. The aim of the present paper is to describe this approach and to demonstrate its efficiency in simulating the membrane insertion of an α -helix by molecular dynamics. The polypeptide we chose for this study is segment 60–105 of glycophorin. This segment contains a region of about 20 hydrophobic residues flanked by two more hydrophilic regions of about 10 residues each [13] *. The membrane incorporation of the hydrophobic segment has been demonstrated by photoreactive labeling [15]. It is supposed to form a membrane-spanning α -helix as

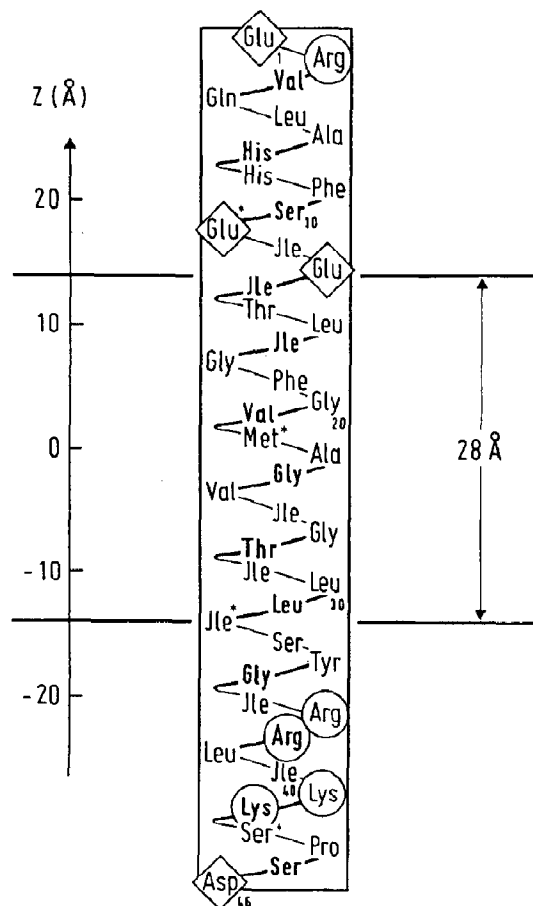


Fig. 1. Schematic model for segment 60–105 of glycophorin folded into an α -helix. The residues have been renumbered 1–46. Circles and diamonds indicate positively and negatively charged residues, respectively. Asterisks denote residues predicted to be at the beginning of a β -turn (according to a Chou-Fasman [37] analysis). The position of the helix in the Z-direction was chosen such that the most hydrophobic segment (according to a Kyte-Doolittle [1] analysis) spans the hydrophobic membrane core of thickness 28 Å.

shown in fig. 1. No prediction can be made on the conformation of the two hydrophilic segments.

Simulating this segment of glycophorin, we also learned what kind of structural fluctuations a membrane-spanning helix can undergo within a time range of 100 ps [16,17]. For a polypeptide of about 50 residues this is the time accessible on a fast computer within a couple of hours of CPU time.

* In a later paper [14] the amino acid sequence of glycophorin was corrected slightly. In segment 60–105 the necessary replacements are: Ile 71 \rightarrow Pro and Gly 77 \rightarrow Ile.

2. Methods

For the MD simulations we used the GROMOS program kindly provided by W. van Gunsteren and H. Berendsen (University of Groningen, The Netherlands). The integration of the classical equations of motion was done with a time step of 2 fs using the SHAKE algorithm to constrain the bond lengths [18]. The temperature was kept at 330 K by coupling the kinetic energy of the system to a heat bath with a relaxation time of 10 fs [19]. This results in fluctuations of the kinetic energy of the order of ± 30 kJ/mol corresponding to temperature fluctuations of the order of ± 8 K. In the case of aliphatic carbon atoms the hydrogens are subsumed under the carbon atoms. The potential energy was described as a sum of the following interaction terms

$$V = V_{\text{angle}} + V_{\text{dihedral}} + V_{\text{Hbond}} + V_{\text{Coul}} + V_{\text{LJ}} + V_{\text{hphobic}} \quad (1)$$

For the first five terms expressions and parameters were taken from the work of Van Gunsteren and Karplus [20]. For the nonbonded interactions (Coulomb and Lennard-Jones) a sharp cut-off at 13 Å was used and a neighbor list specifying the interacting atoms was updated every 10 steps. The fractional charges were chosen to give electroneutral residues, including Lys, Arg, Glu and Asp. Care was taken to avoid splitting of electroneutral groups by the cut-off. Then the long-range electrostatic interactions decay as dipole-dipole interactions. For the hydrogen bonds the cut-off was chosen to be 5 Å and the neighbor list was updated every 20 steps. Since the polypeptide atoms may form hydrogen bonds with water molecules, the hydrogen bond potential was switched off outside the membrane.

To describe the hydrophobic effect we attributed an energy h_i to each atom which is defined as the difference of its free energies in lipid and in water. The values we used are listed in table 1. They were determined to obtain a fair agreement with the experimental hydrophobicities of amino acids obtained by Fauchère and Pliska [21], as demonstrated in table 2 [22]. Compared to the different hydrophobicity scales which have been

Table 1

Hydrophobic energies of atoms

Atom	h (kJ/mol)
H hydrogen	0
S sulfur	0.84
C C_α in peptide	0.43
C aromatic	-1.26
CH1 aliphatic CH	-0.67
CH2 aliphatic CH_2	-1.67
CH3 aliphatic CH_3	-2.80
N in peptide bond	0.84
N terminal in Asn and Gln	0.84
N terminal in Lys	12.34
N terminal in Arg (NH and NH_2)	3.35
N aromatic in His and Trp	2.93
O carbonyl oxygen (C=O)	1.67
O hydroxyl oxygen	1.67
O carboxyl oxygen	3.14

proposed, our values are relatively low. The ordering of water molecules around an atom or molecule is generally considered as the main source of the hydrophobic effect [8]. Furthermore, the ordering of water molecules in front of a mem-

Table 2

Hydrophobic energies of amino acid side chains derived from table 1 and experimental values of Fauchère and Pliska [20] (values in their table III multiplied by $2.3kT$)

Residue	h (kJ/mol)	h_{exp} (kJ/mol)
Gly	-1.00	0
Ala	-2.80	-1.76
Val	-6.27	-6.95
Leu	-7.94	-9.71
Ile	-7.94	-10.29
Pro	-5.01	-4.10
Cys	-0.83	-5.61
Met	-5.30	-7.03
Thr	-1.80	-1.46
Ser	0	0.21
Phe	-9.23	-10.21
Trp	-8.82	-12.84
Tyr	-7.56	-5.48
Asn	2.31	3.43
Gln	0.64	1.26
Asp	5.03	4.39
Glu	3.36	3.64
His	0.41	0.75
Lys	5.66	5.65
Arg	5.47	5.73
Backbone	2.27	-

brane seems to vary exponentially as indicated by measurements of the short-range repulsion between membranes [23,24]. Therefore, we assumed the hydrophobic potential to vary exponentially across the membrane surfaces

$$V_{\text{hydrophobic}} = \begin{cases} \frac{1}{2} \sum_{i=1}^N h_i e^{-(|Z_i| - Z_0)/\lambda} & \text{for } |Z_i| \geq Z_0 \\ \frac{1}{2} \sum_{i=1}^N h_i [2 - e^{(|Z_i| - Z_0)/\lambda}] & \text{for } |Z_i| \leq Z_0. \end{cases} \quad (2)$$

The membrane surfaces are at $\pm Z_0$ and according to this definition specify the hydrophobic core of the membrane. Its thickness is about 30 Å corresponding to $Z_0 = 15$ Å. For the decay length λ we chose 2 Å [23].

The MD simulations were performed on a CRAY-1 supercomputer. One time step took approx. 0.3 s so that a 100 ps run required about 4 h CPU time.

The stereo pictures were produced on an Evans and Sutherland system using the graphics program MIDAS [25].

3. Results and discussion

Using standard potentials for the interactions within a protein and the continuum approximation (eq. 1) for the hydrophobic effect, we performed MD simulations of the 46-residue polypeptide depicted in fig. 1. In a first run we started from a regular α -helix inserted into the membrane with the hydrophobic segment spanning the membrane along the normal. As seen from the stereo pictures of fig. 2 the helical conformation and the membrane insertion are roughly stable over 100 ps. It is also obvious, however, that the polypeptide undergoes some conformational and orientational changes during that time. In the following, we will first elaborate further on the stability of the membrane insertion and then return to the structural changes.

If the membrane incorporation of the hydrophobic segment corresponds to an equilibrium

state, i.e., a global energy minimum and not a local one, then it should also be reached from different initial states. To verify this we performed two simulations with the regular helix initially shifted up or down by 7 Å relative to the membrane. As shown in fig. 3, during the MD run the helix moves back and after 60 ps the hydrophobic segment is incorporated into the membrane as in the unshifted case. Fig. 4 shows the movement of the center of mass of the polypeptide into the membrane together with the accompanying decrease of the hydrophobic energy which is of the order of 20 kJ/mol. This correlation implies that the insertion of the hydrophobic segment into the membrane is a deterministic effect.

When the shifted helix has moved back into its equilibrium position, the N-terminal helix lies flat on the membrane as already observed in the simulation of the unshifted helix (fig. 2). This behavior of the N-terminal helix may be interpreted as a consequence of its amphipathic character. One side of the N-terminal helix made of Leu 5, Ala 6, Phe 9 and Ile 12 is rather hydrophobic and, therefore, prefers to be in contact with the membrane. Although the absorption of the N-terminal amphipathic helix to the membrane surface was found in all our simulations and therefore may represent a deterministic effect, we cannot exclude the possibility that it is a thermal fluctuation.

The conformations which the polypeptide adopts upon moving back into the membrane from above or below differ somewhat. In the first case (fig. 3A), the regular helix becomes banana-shaped, in the second (fig. 3B), the helix is still regular up to the upper membrane surface where a distinct kink occurs so that the N-terminal segment lies flat on the membrane surface. Interestingly, the second case corresponds to the biosynthetic insertion of glycophorin into the red cell membrane. Obviously, in this case it is easy for the membrane-spanning segment to remain a regular α -helix. Whether such a helix would also reform after a longer time in the other case is an open question at this stage.

The same problem was encountered in another simulation when we started from an extended conformation of the polypeptide, 16 nm long, but still inserted into the membrane with the center of

the hydrophobic segment in the middle of the membrane. Within the simulation time of 60 ps all residues of the hydrophobic segment became incorporated into the membrane as in the case of the helix above. However, the helical conformation was not established within this time even when the helix was nucleated with two turns. Hence, our description of the hydrophobic effect leads to a stable insertion of hydrophobic residues

into the membrane in the sense of a true equilibrium state. To form an α -helix takes more time.

In the simulations discussed up to now we used a dielectric constant of unity inside and outside the membrane. To get an idea about the effect of a higher dielectric constant outside the membrane we performed a simulation using $\epsilon = 1$ inside and $\epsilon = 20$ outside the membrane and introducing mirror charges to treat the interface correctly. The

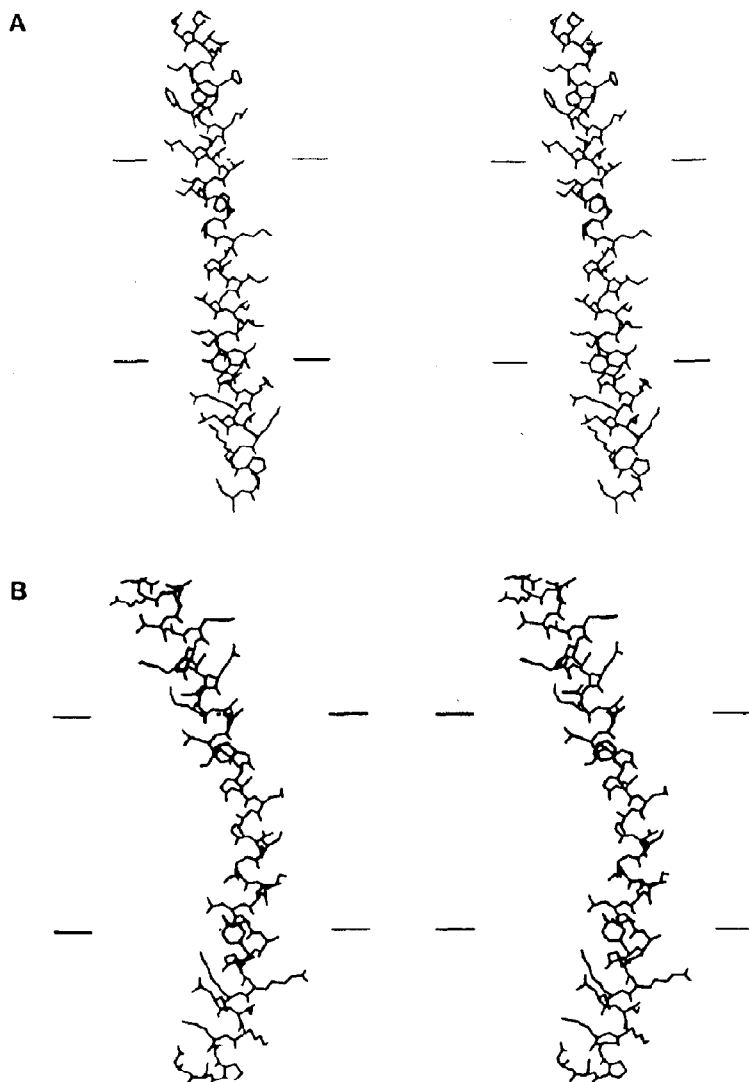


Fig. 2. Stereo pictures of the polypeptide structure at time 0 (A) and after 20 ps (B), 40 ps (C), 60 ps (D), 80 ps (E), and 100 ps (F, here the coordinates have been rotated by 90° relative to the other cases). The straight lines indicate the boundaries of the hydrophobic membrane core of thickness 28 Å.

results after 17 ps is shown in fig. 5. The initial helix has unfolded and a more globular structure is found which is located completely in the membrane.

This insertion of the entire polypeptide into the membrane is a consequence of the electrostatic interactions. In any system containing a mixture of positive and negative charges with enough freedom to move, the electrostatic energy will be negative, i.e., attractive interactions dominate. If some of the interacting charges are moved from outside to inside the membrane, the electrostatic interactions become stronger and the electrostatic

energy becomes more negative. Hence, the entire polypeptide moves into the membrane. The reason for this erroneous result lies in the excessively strong shielding of charges of the polypeptide outside the membrane. This shielding would require water molecules to be present between the charges which usually is not the case, the space between two charges normally being filled with other atoms of the polypeptide. Thus, even outside the membrane it is the dielectric constant of the protein which matters and not that of the surrounding water. We chose $\epsilon = 1$ as the value for this dielectric constant, since the fractional charges

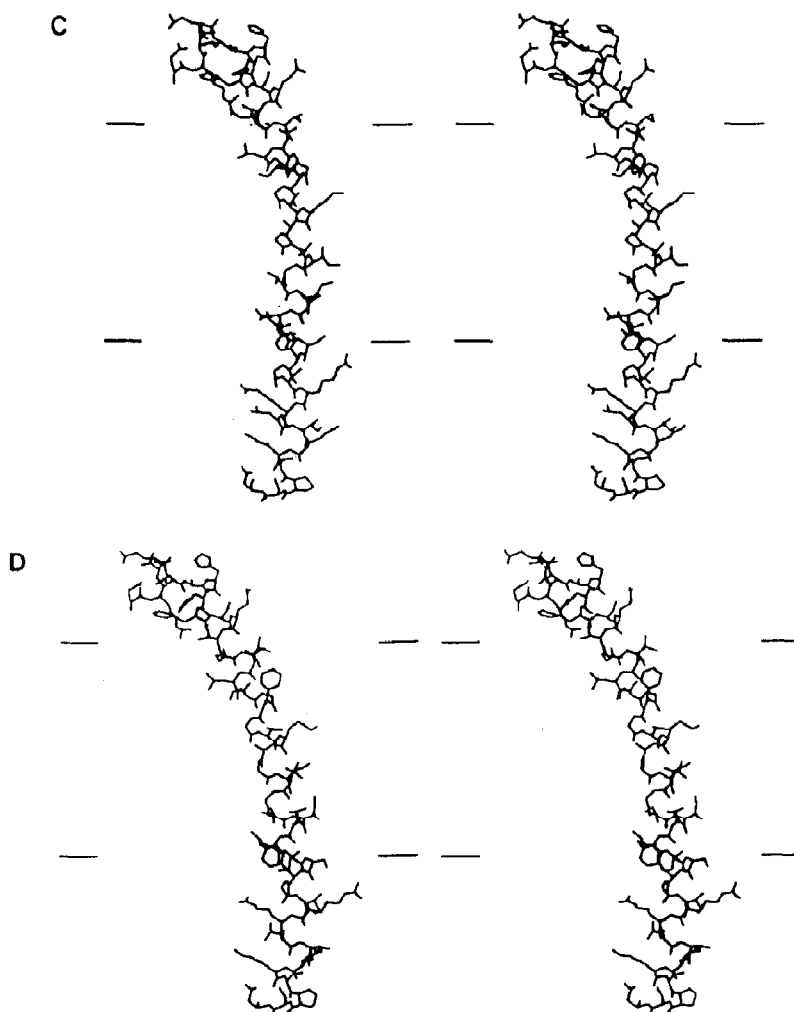


Fig. 2 (C,D).

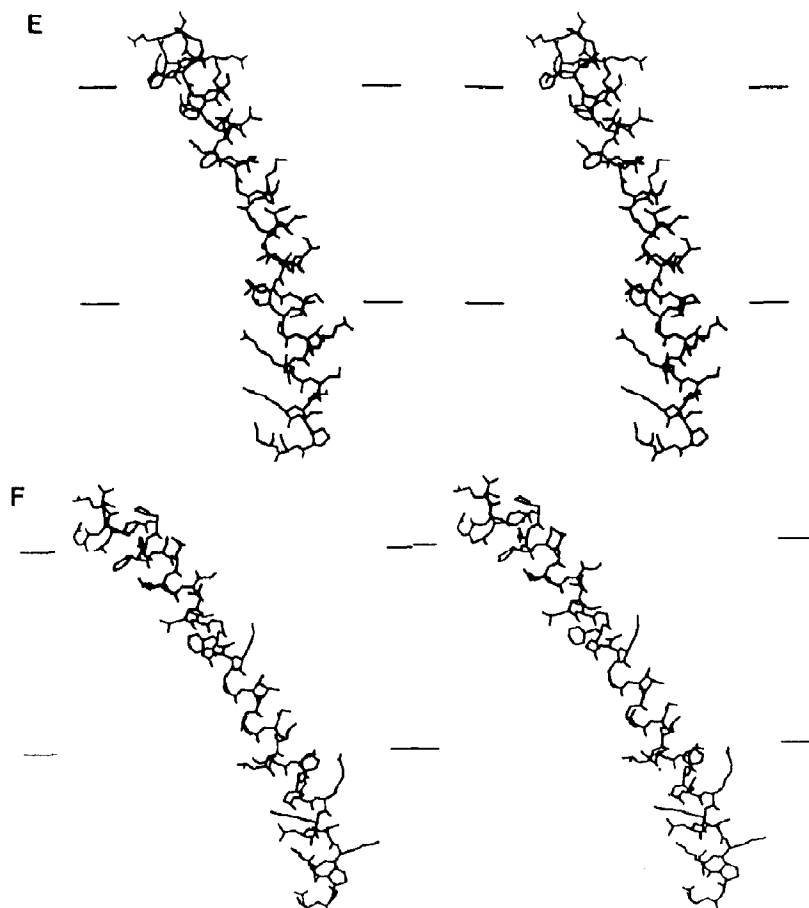


Fig. 2 (E,F).

used had been adjusted to that value. This is a simplified treatment but is completely analogous to the case of soluble proteins. There, several proposals were made to improve the treatment of electrostatic interactions but a final solution of the problem has not yet been obtained [20,26,27]. Hence, it is not worth trying other values of ϵ outside the membrane and the above simulation with $\epsilon = 20$ was performed not in an attempt to improve the description but to demonstrate an unrealistic case.

Returning to the structural changes which the helix undergoes within 100 ps, it should first be noted that none of these changes appeared in an energy minimization of 500 steps. After 20 ps of an MD run, however, the helix has become bent in

the middle. More exactly, two bends have developed, one around Met 22 and another around Leu 31, so that both terminal segments are tilted by about 20° with respect to the membrane normal. After 40 ps, the upper bend has moved towards the upper membrane boundary and is now around Phe 19, while the lower bend has disappeared. From Phe 19 to the C-terminus the polypeptide chain forms a rather regular helix. The N-terminal peripheral segment has partially unfolded and adopted a more globular structure while approaching the membrane boundary. After 60 ps, this segment is lying on the membrane surface and after 80 ps has partially entered the membrane. Concomitantly, the membrane-spanning helix has become more tilted, the tilt angle reaching 35° .

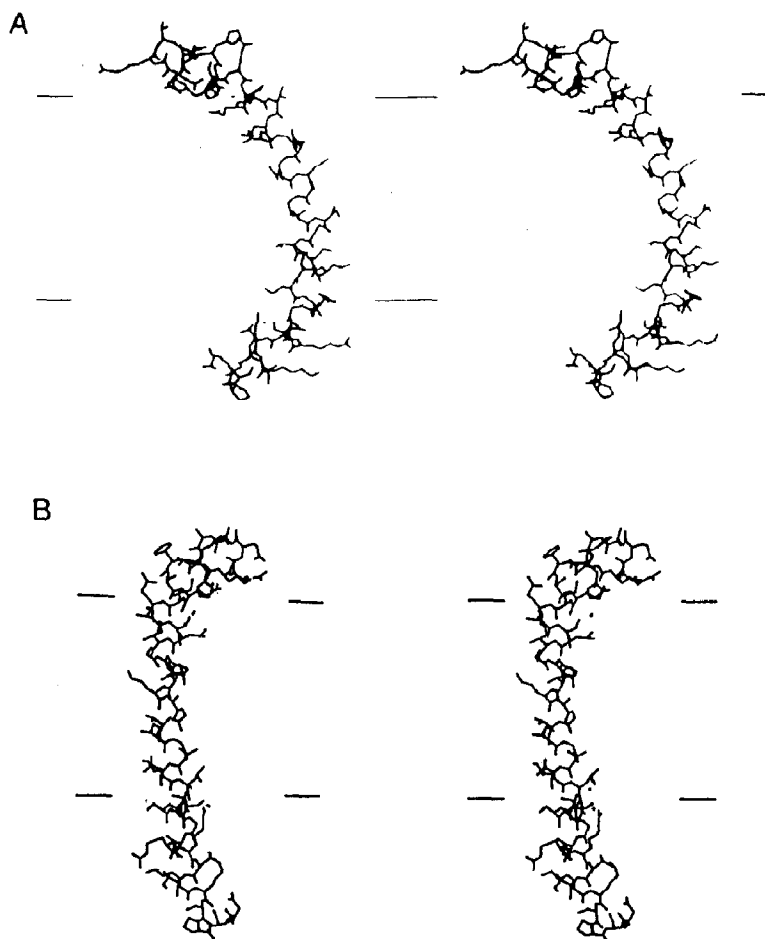


Fig. 3. Stereo pictures of the polypeptide structure in a membrane of core thickness 28 Å after 60 ps when initially the regular helix was shifted up (A) or down (B) by 7 Å relative to the membrane.

Since the C-terminal peripheral segment does not undergo a change in conformation or orientation, a bend appears near the lower membrane boundary, around Leu 31. After 100 ps, this bend has disappeared and the C-terminal segment lies parallel to the membrane-spanning helix. Thus, after 100 ps the polypeptide chain again forms a rather regular α -helix as at the beginning, but the helix is now tilted by about 30°.

The temporal behavior of the tilt of the membrane-spanning helix is shown in fig. 6 where we have plotted the distance between Glu 13 and Ile

32 – those residues which mark the ends of the hydrophobic segment – and the projection of this distance onto the membrane normal. Up to 40 ps, both lengths essentially agree which means no tilt, but after 60 ps the projected length decreases, indicating increased tilt. At 80 ps, the projected length passes through a minimum and the corresponding tilt angle becomes 35°. At 100 ps, the tilt angle has again decreased to about 30°.

On the basis of these data it is not possible to decide whether the tilt is a deterministic effect or just a thermal fluctuation. Therefore, we con-

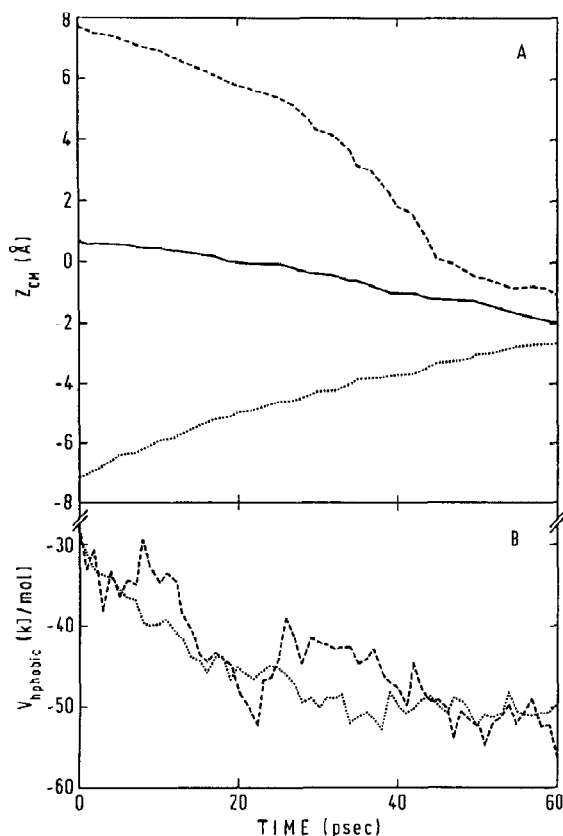


Fig. 4. Temporal variation of the center of mass (A) and of the hydrophobic energy (B) of the polypeptide in a membrane of core thickness 28 Å when initially the regular helix was unshifted (—), shifted up (-----), or shifted down (·····) by 7 Å relative to the membrane.

tinued the MD run to 200 ps. After 100 ps, the tilt again starts to decrease and levels off at about 45°. This result indicates that the tilt is a de-

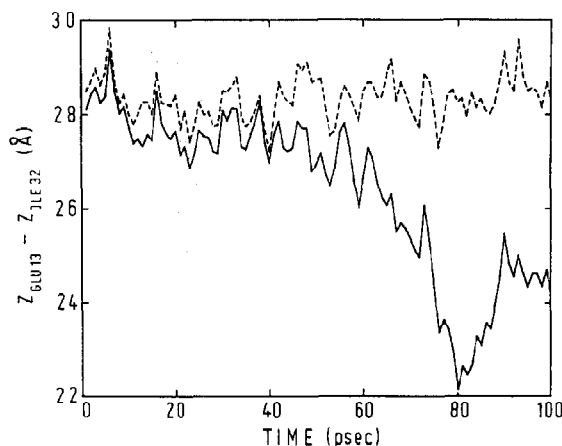


Fig. 6. Temporal variation of the distance between the C_α atoms of Glu 13 and Ile 32 (-----) and of the projection of this distance onto the membrane normal (—). Membrane core thickness 28 Å.

terministic effect. It should be noted, however, that in the presence of lipid molecules the tilt would probably be smaller. A tilt angle of about 20° was observed in a simulation of the membrane-spanning segment of the same helix with explicit treatment of lipid molecules [7].

Upon closer inspection, the two curves of fig. 6 reveal an oscillation of the length of the membrane-spanning helix with a period of 4–5 ps and an amplitude of the order of ± 0.5 Å. A more careful analysis of this oscillation could be given in terms of the autocorrelation function of the helix length $g_l(t) = \langle \Delta l(t) \Delta l(0) \rangle$ with $\Delta l(t) = l(t) - \langle l \rangle$. Unfortunately, the statistical accuracy of our calculation is not sufficient to deduce the period of the oscillation from the time behavior of

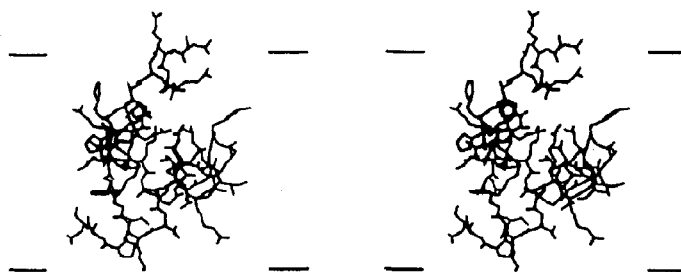


Fig. 5. Stereo picture of the polypeptide structure after 17 ps in a membrane of core thickness 28 Å with $\epsilon=1$ inside and $\epsilon=20$ outside the membrane core.

$g_i(t)$, since the value of $g_i(t)$ has dropped down to the noise level already after 2 ps. What can be determined with some reliability is the mean-square deviation $g_i(0) = \langle (\Delta I)^2 \rangle$ yielding the standard deviation $\sigma_i = g_i(0)^{1/2}$. For the membrane-spanning helix we obtained $\sigma_i = 0.47$ Å. A similar result has been obtained by Levy et al. [28] in MD simulations of a decaglycine helix.

This oscillation reflects an accordion-like vibration of the membrane-spanning helix. Peticolas [29] investigated such vibrations by modeling the helix as a series of masses and springs. His result for the frequency of the oscillation is

$$\nu = 2\nu_0 \sin\left(\frac{3.6\pi}{2n}\right) \quad (3)$$

with n denoting the number of residues in the helix and $\nu_0 = 1.05 \times 10^{12} \text{ s}^{-1}$ for an average mass of 110 Da per residue. He also calculated the standard deviation σ_i and obtained to a very good approximation a linear increase of σ_i with n . Insertion of our MD value $\sigma_i = 0.47$ Å for the membrane-spanning helix into his result leads to $n = 22$ in agreement with the actual length of this helix. Using this length of $n = 22$ to derive the frequency ν or period $T = 1/\nu$ from eq. 3, one obtains $T = 1.9$ ps, while with the total length of $n = 46$ one obtains $T = 3.9$ ps. The latter value is in agreement with our experimental result which indicates that the entire helix participates in the accordion-like oscillation, and not only the membrane-spanning segment.

Fig. 7 shows plots of the backbone angles ϕ and ψ of residue Met 22 as functions of time. For other residues, except the last five at both termini, the angles behave similarly. Over the entire 100 ps of the run they undergo fluctuations of $\pm 20^\circ$ about the values for a right-handed α -helix which are $\phi = -58^\circ$ and $\psi = -48^\circ$. Hence, the bending of the helix seen in fig. 2 is not easily detected in the backbone angles. This is because the bending is distributed over several neighboring angles and the change in each individual angle is small compared to its thermal fluctuation. Fig. 7 furthermore reveals that the fluctuations of ϕ and ψ are usually anticorrelated. Therefore, they are not accompanied by large conformational changes. Nevertheless, bending seems not to be completely

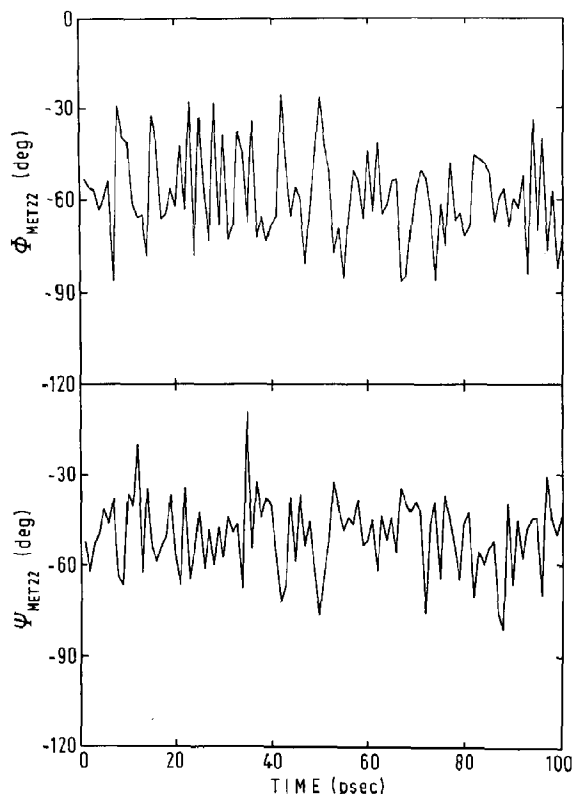


Fig. 7. Temporal variation of the torsion angles ϕ and ψ of Met 22. Membrane core thickness 28 Å.

random. There are only three regions where a large degree of bending occurs: near Glu 11, Met 22 and Ile 32. The first and last regions are just at the ends of the hydrophobic segment and thus are located at the membrane surface. Met 22 lies in the middle of the hydrophobic segment. Here, bending always occurs towards that side of the helix which is marked by the nonbulky residues Gly 20, Ala 23 and Gly 24, so that steric reasons are responsible for the bend. In the other two cases, the reason for the bend is not as obvious. Interestingly, however, the Chou-Fasman rules predict β -turns for all three regions of bend (fig. 1). Hence, these regions seem to be favored for bending in a deterministic manner.

In trying to understand why the helix tilts, the first idea which comes to mind is that the membrane is too thin. In the simulation of fig. 2 the membrane is 28 Å thick; if this is not sufficient to

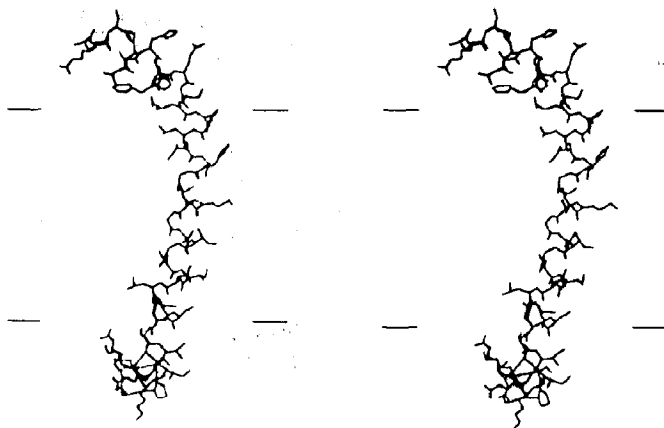


Fig. 8. Stereo picture of the polypeptide structure after 25 ps in a membrane of core thickness 30 Å.

accommodate the hydrophobic segment of the helix in an orientation parallel to the membrane normal, the helix will tilt. Therefore, we increased the membrane thickness to 30 Å and performed another MD run. In the initial configuration, approximately one more residue on each side of the hydrophobic segment is now located inside the membrane. After 15 ps, the structure of the polypeptide is similar to that after 20 ps in the membrane of 28 Å thickness: the helix has a bend in the middle of the membrane. After 25 ps, as shown in fig. 8, the membrane-spanning segment is a tilted α -helix with bends at both ends. Hence, this simulation does not provide any evidence for a correlation between tilt and membrane thickness.

The tilt might instead be caused by the observed tendency of the N-terminal segment to lie flat on the membrane. If the helix were absolutely stiff, tilting of the N-terminal segment would require tilting of the entire helix. However, as discussed above, at both ends of the membrane-spanning segment one finds a pronounced tendency for a bend or turn. Hence, the orientation of the outer segments does not seem to be strongly coupled with the orientation of the membrane-spanning segment and the N-terminal segment may well lie on the membrane while the membrane-spanning helix undergoes orientational fluctuations.

In fig. 9 we have plotted the total potential energy as a function of time. One cannot observe

any systematic change of the energy during a period of 100 ps. Instead, the energy undergoes fast fluctuations of the order of ± 50 kJ/mol. These fluctuations may seem to be large but are in fact necessary for obtaining a reasonable value for the specific heat of the polypeptide as will be shown. Hence, the structural changes occurring during 100 ps, bending and tilting of the helix, represent thermal fluctuations around an equilibrium structure and not a deterministic change towards an energy minimum.

Formulas relating the energy to the specific heat are available for a canonical and a microcanonical ensemble [30]. Due to the coupling of the kinetic energy to a heat bath, our system is

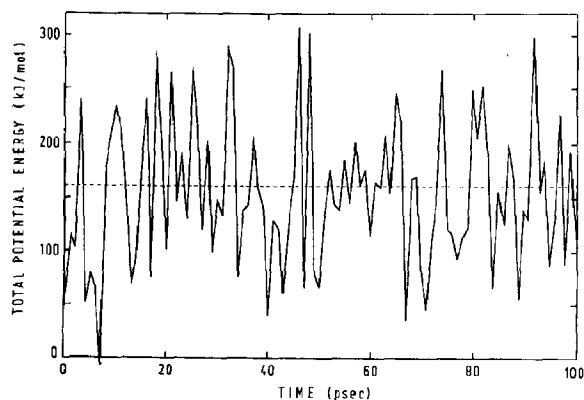


Fig. 9. Temporal variation of the total potential energy of the polypeptide in a membranes of core thickness 28 Å.

Table 3

Contributions of the individual potential energies together with their standard deviations in three different MD simulations

The standard deviations were calculated from the standard deviations of the averages over 5 ps, thus eliminating the short-time fluctuations. Values expressed in kJ/mol.

Simulation	V_{angle}	V_{dihedral}	V_{Hbond}	V_{Coul}	V_{LJ}	$V_{\text{hydrophobic}}$	V_{tot}
28 Å, nonshifted, 100 ps	1283 ± 12	371 ± 9	-130 ± 12	-537 ± 9	-72 ± 19	-50 ± 2	867 ± 22
30 Å, nonshifted, 25 ps	1286 ± 14	369 ± 9	-142 ± 19	-522 ± 22	-39 ± 32	-53 ± 2	898 ± 24
28 Å, shifted 7 Å, 60 ps	1267 ± 23	372 ± 7	-112 ± 16	-502 ± 25	-28 ± 33	-45 ± 7	951 ± 38

closer to a canonical than a microcanonical ensemble. In this case the relevant formula is

$$g_E = kT^2 C_V \quad (4)$$

with $g_E = \langle (\Delta E)^2 \rangle$ denoting the fluctuations of the total energy and C_V the specific heat. In our simulation we obtained $\sigma_E = g_E^{1/2} = 66$ kJ/mol, which using eq. 4 yields $C_V = 4.8$ kJ/mol per degree or with a molecular weight of 5000 for our polypeptide $C_V = 0.96$ J/g per degree. This value agrees fairly well with experimental data for the specific heat of soluble proteins which lie within the range 1.2–1.5 J/g per degree [31].

The individual potential energies behave in a similar way to the total potential energy. This is indicated in table 3, which lists the mean values of the individual energies averaged over the final 5 ps of different simulations together with their standard deviations. The standard deviations here are smaller than those given above for the total energy, since they were calculated from the standard deviations of the averages over 5 ps, thereby eliminating the short-time fluctuations. The hydrophobic energy shows exceptionally small fluctuations of the order of thermal energy. This indicates that translation perpendicular to the membrane is not strongly coupled to the internal degrees of freedom of the polypeptide, i.e., the membrane insertion of a hydrophobic polypeptide

is stable, independently of conformational fluctuations.

4. Conclusions

Our MD simulations demonstrate that the membrane insertion of a hydrophobic segment of amino acids can be well described by a continuum approximation for the water and lipid phase using phenomenological energies for the hydrophobic effect of the polypeptide atoms. At the same time, a dielectric constant of unity for the electrostatic interactions within the polypeptide should be used. As stated in section 1, by making use of phenomenological hydrophobic energies one avoids the calculation of the small difference between the large interactions of the atoms of a polypeptide with water and lipid. The choice of $\epsilon = 1$ parallels the case of soluble proteins and accounts for the fact that most of the electrostatic interactions between atoms of the polypeptide are not shielded by atoms of water.

Since our approach is basically a simulation in a vacuum, although the lipid/water interface is taken into account, it does possess some shortcomings. First, interactions within the polypeptide are overestimated due to the lack of surrounding lipid and water molecules. This might lead to a smoother surface of the polypeptide than in reality. Second, bending and tilting of membrane-spanning helices may turn out to be too large. Third, much of the dynamics of the polypeptide may be too fast, e.g., wobbling fluctuations of membrane-spanning helices or rotational diffusion about their long axes.

* The numbers for σ_E are given in units of energy per mol protein. This would correspond to the case where all protein molecules fluctuate in synchrony which is unrealistic. Actually, σ_E is proportional to $N^{1/2}$ and the relative fluctuations σ_E/E decrease proportionally to $N^{-1/2}$, becoming vanishingly small for a macroscopic system.

The hydrophobic energy of a membrane-spanning segment is small relative to the internal energy of the segment, but is comparable to the thermal fluctuations of the internal energy. This might have the consequence that the hydrophobic effect would be hidden by the internal fluctuations of the segment. However, this is not the case, the internal degrees of freedom not being strongly coupled with the center of mass motion into and out of the membrane. Therefore, the relatively small hydrophobic energy is sufficient to guarantee stable membrane insertion of a hydrophobic segment which itself undergoes strong internal fluctuations. This also justifies the use of a rather simple description for the hydrophobic effect in connection with a detailed MD simulation of the polypeptide conformation.

The internal fluctuations of a membrane-spanning segment involve large fluctuations in energy, but not large conformational changes. The conformation of a membrane-spanning segment is α -helical due to the requirement of forming hydrogen bonds intramolecularly and as such does not change. The helix may, however, undergo fluctuations in bending and in length. In addition, a membrane-spanning segment may also exhibit orientational fluctuations about the membrane normal. Thus, the orientational fluctuations of an individual residue on a membrane-spanning helix are a superposition of the wobbling motion of the helix and bending fluctuations which may vary along the helix. This is analogous to the orientational fluctuations of lipid molecules which are also a superposition of a wobbling motion and conformational fluctuations [6,32]. Orientational fluctuations of amino acid side chains in a membrane-spanning helix appear to have been observed recently by fluorescence anisotropy decay measurements [33,34].

Unfortunately, from our MD simulations we cannot say much about the temporal behavior of these fluctuations. Evidently, they are not of the oscillatory type as are the fluctuations in helix length. The period of oscillating fluctuations can be calculated quite reliably by MD simulations, but the characteristic time of relaxing fluctuations is difficult to determine because (i) the time range of 100 ps is too small, (ii) damping is described in

a very crude approximation by coupling the kinetic energy to a heat bath, and (iii) lipid molecules are not treated explicitly. The fluorescence anisotropy decay measurements mentioned above yielded relaxation times in the range of 10–100 ns for the orientational fluctuations of a membrane-spanning helix [33,34].

The coexistence of fast and slow fluctuations – fluctuations of the helix length and fluctuations of bending and tilting – is consonant with a general scheme for the dynamics of proteins which has been proposed recently [35]. Here, the fluctuations obey a hierarchical order. A fast fluctuation which occurs in a valley of the energy gives rise, from time to time, to a transition across an energy barrier and thus induces a slower fluctuation. Such a slow fluctuation may be functionally important. For example, the bending and tilting fluctuations of a membrane-spanning helix in a transport protein may well play a role in transport [36]. Thus, if one were to succeed in calculating the equilibrium structure of a transport protein by MD simulations, the fluctuations obtained at the same time would provide insight into the mechanism of transport.

Acknowledgments

We thank W. van Gunsteren and H. Berendsen from the University of Groningen for allowing us to use the GROMOS program and J. Postma from the EMBL at Heidelberg for his help in producing the stereo pictures. This work was supported by the Swedish National Science Research Council in the form of a grant to O.E. (K-KU 3777-104) and allotment of computer time on a CRAY-1, and by EMBO in the form of a short-term fellowship to F.J. (ASTF 4938).

References

- 1 J. Kyte and R.F. Doolittle, *J. Mol. Biol.* 157 (1982) 105.
- 2 F. Jähnig, in: *Prediction of protein structure and the principles of protein conformation*, ed. G.M. Fasman (Plenum Press, New York, 1988) in the press.
- 3 M. Karplus and J.A. McCammon, *Annu. Rev. Biochem.* 53 (1983) 263.

- 4 A.T. Brünger, G.M. Clore, A.M. Gronenborn and M. Karplus, *Proc. Natl. Acad. Sci. U.S.A.* 83 (1986) 3801.
- 5 W.F. van Gunsteren, H.J.C. Berendsen, J. Hermans, W.G.J. Hol and J.P.M. Postma, *Proc. Natl. Acad. Sci. U.S.A.* 80 (1983) 4315.
- 6 P. van der Ploeg and H.J.C. Berendsen, *Mol. Phys.* 49 (1983) 233.
- 7 O. Edholm and J. Johansson, *Eur. Biophys. J.* 14 (1987) 203.
- 8 C. Tanford, *The hydrophobic effect* (Wiley, New York, 1980).
- 9 F. Jähnig, *Proc. Natl. Acad. Sci. U.S.A.* 80 (1983) 3691.
- 10 M. Neumann, *J. Chem. Phys.* 82 (1985) 5663.
- 11 K. Watanabe and H.C. Andersen, *J. Phys. Chem.* 90 (1986) 795.
- 12 B. Jönsson, O. Edholm and O. Teleman, *J. Chem. Phys.* 85 (1986) 2259.
- 13 M. Tomita and V.T. Marchesi, *Proc. Natl. Acad. Sci. U.S.A.* 72 (1975) 2964.
- 14 M. Tomita, H. Furthmayr and V.T. Marchesi, *Biochemistry* 22 (1978) 4756.
- 15 A.H. Ross, R. Radhakrishnan, J.J. Robson and H.G. Khorana, *J. Biol. Chem.* 257 (1982) 4152.
- 16 A.T. Hagler, D.J. Osguthorpe, P. Dauber-Osguthorpe and J.C. Hempel, *Science* 227 (1985) 1309.
- 17 D.H.J. MacKay, P.H. Berens, K.R. Wilson and A.T. Hagler, *Biophys. J.* 46 (1984) 229.
- 18 J.P. Ryckaert, G. Ciccotti and H.J.C. Berendsen, *J. Comp. Phys.* 23 (1977) 327.
- 19 H.J.C. Berendsen, J.P.M. Postma, W.F. van Gunsteren, A. Dinola and J.R. Haak, *J. Chem. Phys.* 81 (1984) 3684.
- 20 W.F. van Gunsteren and M. Karplus, *Macromolecules* 15 (1982) 1528.
- 21 J.L. Fauchère and V. Pliska, *Eur. J. Med. Chem. Chim. Ther.* 18 (1986) 369.
- 22 D. Eisenberg and A.D. McLachlan, *Nature* 319 (1986) 199.
- 23 V.A. Parsegian, N. Fuller and R.P. Rand, *Proc. Natl. Acad. Sci. U.S.A.* 76 (1979) 2750.
- 24 J. Israelachvili and R. Pashley, *Nature* 300 (1982) 341.
- 25 R. Longridge, T.E. Ferrin, I.D. Kuntz and M.L. Connolly, *Science* 211 (1981) 661.
- 26 M.K. Gilson, A. Rashin, R. Fine and B. Honig, *J. Mol. Biol.* 183 (1985) 503.
- 27 S.T. Russell and A. Warshel, *J. Mol. Biol.* 185 (1985) 389.
- 28 R.M. Levy, D. Perahia and M. Karplus, *Proc. Natl. Acad. Sci. U.S.A.* 79 (1982) 1346.
- 29 W.L. Peticolas, *Biopolymers* 18 (1979) 747.
- 30 J.L. Lebowitz, J.K. Percus and L. Verlet, *Phys. Rev.* 153 (1967) 250.
- 31 A. Cooper, *Proc. Natl. Acad. Sci. U.S.A.* 73 (1976) 2740.
- 32 L. Best, E. John and F. Jähnig, *Eur. Biophys. J.* 15 (1987) 87.
- 33 K. Dommair and F. Jähnig, in: *Spectroscopy of biological molecules*, eds. J.P.M. Alix, L. Bernard and M. Manfait (Wiley, New York, 1985) p. 291.
- 34 H. Vogel and R. Rigler, in: *Structure, dynamics and function of biomolecules*, eds. A. Ehrenberg, R. Rigler, L. Nilsson and A. Gräslund (Springer, Berlin, 1987) p. 289.
- 35 A. Ansari, J. Berendzen, S.F. Bowne, H. Frauenfelder, I.E.T. Iben, T.B. Sauke, E. Shyamsunder and R.D. Young, *Proc. Natl. Acad. Sci. U.S.A.* 82 (1985) 5000.
- 36 O. Jardetzky, *Nature* 211 (1966) 969.
- 37 P.Y. Chou and G.D. Fasman, *Annu. Rev. Biochem.* 47 (1978) 251.